Article ID: 1001-3555(2020)01-0045-13

Highly Selective Synthesis of Trans-1-Chloro-3,3,3-Trifluoropropene by the Vapor Fluorination of 1,1,3,3-Tetrachloropropene with HF over the Chromium Oxide-Based Catalysts

TIAN Mi[1,3], GAO Ping[2], ZHANG Rong-hui[1,3], WANG Lai-lai[1*], ZHOU Wang-ying[4], XIE Wen-jian[4]

(1. *State Key Laboratory for Oxo Synthesis and Selective Oxidation*, *Lanzhou Institute of Chemical Physics*, *Chinese Academy of Sciences*, *Lanzhou* 730000, *China*;

2. *State Key Laboratory of Solid Lubrication*, *Lanzhou Institute of Chemical Physics*, *Chinese Academy of Sciences*, *Lanzhou* 730000, *China*;

3. *Graduate University of Chinese Academy of Sciences*, *Beijing*, 100039, *China*;

4. *Lee & Man Chemical Company Limited*, *Jiangsu* 215536, *China*)

Abstract: Vapor fluorination of 1,1,3,3-tetrachloropropene (HCC-1230za) with HF to trans-1-chloro-3,3,3-trifluoropropene (HCFO-1233zd(*E*)) was investigated using the fluorinated Cr_2O_3 catalysts modified by Al^{3+}, Zn^{2+}, and Co^{2+}. A highly active, selective, and long lifespan Zn/Cr_2O_3 catalyst was achieved for the first time, where 99.4% HCC-1230za conversion and 98.2% HCFO-1233zd (*E*) selectivity were obtained, and the selectivity to HCFO-1233zd (*E*) was favored at 200 ℃ and HF/HCC-1230za molar ratio (10∶1). The catalysts were characterized by XRD, XPS, BET, V70 pyridine adsorption infrared spectrometer and NH_3-TPD techniques. The XRD results of catalysts Zn/Cr_2O_3 indicate that most of the amorphous chromium oxide and finely dispersed microcrystalline phase of Cr_2O_3 together lead to high activity and long lifespan. The conversion of HCC-1230za and the selectivity to HCFO-1233zd (*E*) are related to the specific surface area of the fluorinated catalyst, and the higher the specific surface area of the catalyst, the higher selectivity. The XPS spectra of catalyst Zn/Cr_2O_3 show that exterior Cr_2O_3 after 118 h reaction formed CrO_xF_y species. The number and strength of Lewis and Brønsted acid sites for Zn/Cr_2O_3 catalysts after 118 h reaction is significantly increased than the fresh one.

Key words: fluorination; 1,1,3,3-Tetrachloropropene; HF; trans-1-chloro-3,3,3-trifluoropropene; fluorinated chromia

CLC number: O643.36 **Document code**: A

Fluorine-containing hydrocarbons are commonly used as refrigerants, aerosol sprays, and foaming agents[1-3] 1,1,1,3,3-pentafluoropropane (HFC-245fa) as the third generation foaming agent with an atmospheric ozone depletion potential (ODP) of 0, the greenhouse effect potential (GWP) of 1030, faces the reality of being restricted and abandoned[4-6]. Non-flammabletrans-1-chloro-3,3,3-trifluoropropene (HCFO-1233zd (*E*)) with low toxicity under normal conditionsis the fourth generation of blowing agents developed in recent years[7-10]. Its ODP and GWP are 0.000 24 and 7.0 respectively.

More particularly, it is a monomer for synthesizing polymeric materials, and a building block for making other fluorinated compounds. Compared with cis-1-chloro-3,3,3-trifluoropropene (HCFC-1233zd (*Z*)), HCFO-1233zd (*E*) has higher thermos-dynamic stability, and 10% of HCFO-1233zd (*E*) can be isomerized to HCFC-1233zd (*Z*) at 300 ℃ using fluorinated Cr_2O_3 catalysts[11].

HCFO-1233zd (*E*) was synthesized in liquid phase fluorination of 1,1,1,3,3-pentachloropropane (HCC-240fa) with HF using Lewis acid catalysts[12-17]. However, the target product was synthe-

Received date: 2019-11-17; **Revised date**: 2019-12-12.

Foundation: Key Research Program of Science and Technology Project of Gansu province (No.18YF1GA124).

First author: TIAN Mi(1993-), female, Master candidate.

* **Corresponding author**, E-mail: wll@licp.cas.cn, Tel: +86-931-4968161, Fax: +86 931 4968129.

sized in batches, and the reaction lead to more industrial wast and serious equipment corrosion. Special attention has been paid to vapor fluorination for the synthesis of HCFO-1233zd (*E*) in the chemical industry, because of its potential of industrial continuous production. Until now, only several patents reported vapor fluorination routes to synthsize HCFO-1233zd(*E*)[18-22]. Catalysts such as Cr_2O_3[18], $CrCl_3/Al_2O_3$[19], AlF_3[20-21] and Cr-Ni/AlF_3[22] are used to reach the conversion of HCC-240fa of 100%, and the selectivity of HCFO-1233zd (*E*), and catalyst lifespan are not ideal. Merkel et al introduced air into the reactants with the O_2/HCC-240fa molar ratio of 0.032 ∶ 1, the regeneration and activation of the catalyst would be completed, and at least one more lifespan could be extended[23]. The high-valent metal halide-supported catalysts are reported to avoid rapid carbonation on the catalyst surface caused by high temperature and the formation of deep fluorinated by-products[24-26]. Though the yield of the process reached industrial application requirements, this patented technology does not address the stability of the catalyst. In addition, the usage of precious metals such as Sb, Ta, Mo and Nb etc limited the application of this technology.

Though satisfactory selectivity of HCFO-1233zd (*E*) through vapor fluorination of HCC-240fa with HF-has been obtained using Cr_2O_3 fluorination catalyst at 270 ℃ or higher, coke on the catalyst surface accelerates the catalyst deactivation[18,27-29]. We reported highly selective synthetic route to HCFO-1233zd (*E*) by vapor fluorination of 1, 1, 3, 3-tetrachloropropene (HCC-1230za) with HF over the Cr_2O_3-based catalysts. HCC-1230za was synthesized through highly selective dehydrochlorination of HCC-240fa using activated carbon. 99.4% HCC-1230za conversion and 98.2% HCFO-1233zd (*E*) selectivity are obtained at 200 ℃, and the catalyst achieved long lifespan in this reaction.

1 Experimental details

1.1 Catalyst Preparation

The M (M = Zn^{2+}, Co^{2+}, Al^{3+}) modified Cr_2O_3 catalysts were prepared by a precipitation method. A detailed preparation process of the catalyst Zn/Al/Cr_2O_3 is as follows: 6.815 g (0.05 mol) of zinc chloride, 24.15 g (0.1 mol) of aluminum trichloride hexahydrate, and 133.2 g (0.5 mol) of chromium trichloride hexahydrate, Zn^{2+} ∶ Al^{3+} ∶ Cr^{3+} = 0.1 ∶ 0.2 ∶ 1 (mol/mol/mol), dissolved in 270 mL of distilled water. Subsequently, 76 g of NaOH (19 mol/L) was added to a solution of Zn^{2+}, Al^{3+} and Cr^{3+}, and magnetically stirred until precipitation occurred and allowed to stand for 24 hours. The precipitate after aging was filtered and washed with about 2000 mL of distilled water until the pH of the solution is 7~8, then dried at 60 ℃ for 48 h, followed by a calcination at 460 ℃ for 4 h in H_2, and the oxide after calcination was 54.0 g. 3% (Percent weight) of colloidal graphite were added to the calcined oxide, and grounded by a high-speed universal pulverizer. 5%(Percent weight) of methyl cellulose solution was added to the mixture, extruded and formed into cylindrical the final catalysts, and air-dried at room temperature. Preparation process of the catalyst Co/Al/Cr_2O_3(Co^{2+} ∶ Al^{3+} ∶ Cr^{3+} = 0.2 ∶ 0.1 ∶ 1 mol/mol/mol) and Zn/Cr_2O_3(Zn^{2+} ∶ Cr^{3+} = 1 ∶ 36 mol/mol) are basically the same as above.

Zn^{2+}-doped Cr_2O_3 supported over spherical γ-alumina catalyst 4% Zn/2% Cr/γ-Al_2O_3(Percent weight) was prepared as follows: 4.880 g of zinc chloride and 5.930 g of chromium trichloride hexahydrate were dissolved in 58 mL of distilled water, which is used as an immersion liquid; 50 g spherical γ-Al_2O_3 carrier was added to the impregnating solution, followed by evaporating any residual water, then dried at 70 ℃ for 72 h. Spherical γ-Al_2O_3 carrier: Φ5.0 mm, specific surface area ⩾ 300 m^2/g, pore volume ⩾ 0.40 mL/g, bulk density 0.73 ± 0.03 g/mL. Using the same method as above to prepare catalyst 8% Zn/4% Cr/γ-Al_2O_3(Percent weight).

1.2 Catalytic fluorination

HCC-240fa is synthesized by any means well known in the literature[30-32], and the synthesis of HCC-1230za (Scheme 1) is carried out using HCC-240fa as startng material as follow: 160 g of activated carbon is added to the quartz glass tube (1.5 m × 30 mm), using the method of upper feed and lower discharge. In order to ensure the smooth discharge of the

product, a nitrogen purge is introduced during the reaction. The flow rate of nitrogen gas is 10 mL/min, the reaction temperature is controlled at 190~200 ℃, and the product is collected by ice salt bath cooling. During the whole reaction stage, GC analysis using a gas chromatograph (Agilent GC-7890) equipped with a flame ionization detector (FID) and a HP-5 (30 m) capillary column follows the reaction. A total of 3.0 kg HCC-240fa was input, the feed rate was 30 mL/h, and the unreacted HCC-240fa adsorbed by activated carbon was 0.32 kg. The theoretical product should be 2.23 kg, while the actual collected product HCC-1230za was 2.0 kg. The yield is 89.6%, and GC content of HCC-1230za is >94%.

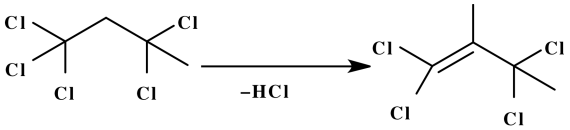

Scheme 1 Highly selective dehydrochlorination of HCC-240fa to HCC-1230za using activated carbon

Activity test of catalyst Zn/Cr_2O_3 is as follows: 10~20 g of the catalyst was filled into 304 stainless steel reaction tube (50 cm×20 mm), heated by tube furnace at 150~300 ℃. Due to the high corrosiveness of HF, the gas tightness of the reaction system needs to be checked during the experiment to prevent HF leakage. Flow rate of HF pre-heated in a chamber at 45 ℃ was carefully controlled at 60 mL/min. Using a sevenstar mass flowmeter. During the activation process, a large amount of water was generated and continuously activated for 10 h. The activation was complete until no water is formed in the reaction tube. Subsequently, HCC-1230za feed was regulated at room temperature with a liquid pump, and the feed amount of HCC-1230za was 0.6 mL/min. The molar ratio of HCC-1230za to HF was detected by acid-base titration, and the ratio was fixed at 1∶10. The fluorination reaction was under normal pressure at 200 ℃. The effluent flow from the reactor was washed with NaOH solution in a scrubber for the removal of HCl and HF, the stream was further dried using NaOH pellets, and then the gaseous products were condensed to obtain a liquid sample for analysis. GC-MS (Thermo Scientific ITQ 700) was applied for identity of the organic compounds formed during the reaction. The reaction products were analyzed by before mentioned gas chromatograph. The relative composition of the products is based on peak areas, therefore do not represent the absolute yields, because of difference in response factors. When the GC content of HCFO-1233zd (*E*) decreased by more than 10%, the catalyst was considered to be deactivated. Activity test of catalyst $Zn/Al/Cr_2O_3$, $Co/Al/Cr_2O_3$, 4% Zn/2% Cr/γ-Al_2O_3, and 8% Zn/4% Cr/γ-Al_2O_3 is basically the same as above.

We selected consecutive three hours as the time node for material balance calculation: the total feed volume was 164.0 g, and the two-stage cooling device collected a total of 98.8 g of crude products and a total input of 164.0 g. The theoretical product yield was 120.3 g, the reaction yield was 82.1%. The crude GC analysis results obtained by the two-stage cooling device contained 0.62% HCC-1230za, 91.2% HCFC-1233zd (E), 1.7% HCC-245fa, and 4.1% difluorodichloropropylene. The material was lost during the reaction. The main reason was that high purity nitrogen was used in the entire experiment to dilute HF concentration to reduce safety risks, and some crude products were blown away by high purity nitrogen.

1.3 Characterization

The catalysts was subjected to crystal phase analysis through PANalytical X'Pert PRO Polycrystalline Powder X-ray diffractometer (Cu Kα, λ = 0.154 18 nm) (PANalytical BV, Almelo, Netherlands) with an angle reproducibility of ±0.0001°, the diffraction data of 2θ in 8°~80° was collected by θ/θ scanning method with a scanning speed of 2°/min. Chemical compositions on the surface of samples were analyzed using an X-ray photoelectron spectrometer (XPS) (Thermo Fisher Scientific ESCALAB 250Xi) equipped with an Al monochromatic X-ray source (Al Kα = 1486.6 eV, C 1*s* was corrected to 284.8 eV) under room temperature in high vacuum (about 1×10^{-9} Pa). The N_2 adsorption-desorption characterization of the samples was performed on a specific surface area analyzer Micromeritics ASAP2020 V3.04 H (Micromeritics Instrument

Co., Ltd., Norcross, USA) at liquid nitrogen temperature (−196 ℃). The specific surface area of the catalyst was determined using the Brunauer-Emmet-Teller (BET) method. The pore size distribution was analyzed by the adsorption-desorption isotherm through the Barret-Joyner-Halender (BJH) method using a columnar pore model.

The Brønsted and Lewis acid site of the sample were determined by V70 pyridine adsorption infrared spectrometer (Bruker, Germany) with a resolution of 4 cm^{-1} and an uptake range of 400 ~ 4000 cm^{-1}. The catalyst sample was pressed into a thin sheet, placed in a quartz infrared cell, heated to 400 ℃ and maintained a constant temperature for evacuation pretreatment, then was degassed and dehydrated under high vacuum (1×10^{-3} Pa) for 2 h, and naturally cooled to 150 ℃. The anhydrous pyridine was adsorbed at 150 ℃ for 30 min, then heated to 400 ℃ to start desorption, 400 ℃ for 0.5 h, 150 ℃ for 0.5 h, and then the Py-IR spectrum was recorded on an infrared spectrometer. The temperature-programmed desorption of ammonica (NH_3-TPD) measurement was carried out on a fully automatic multifunctional dynamic adsorber instrument DAS-7200 (Huasi Instrument Co., Ltd, China) for comparing the acidity strength of the composite catalysts. A sample of 100 mg on the quartz glass tube (i. d. = 5 mm) was first pretreated in pure N_2 from 100 to 450 ℃ at a rate of 10 ℃/ min, and kept at 450 ℃ for 2 h. followed by cooling to 100°C in a flow of N_2 (30 mL/min). NH_3-N_2 mixture (10% NH_3, 30 mL/min) was introduced to the reactor for 2 h. to allow the complete adsorption of NH_3. Prior to measurement, the sample was purged with pure N_2 (30 mL/min) to remove physically absorbed NH_3 for 60 min. Then the sample was heated in the N_2 flow (30 mL/min) from 100 to 850 ℃ with a heating rate of 10 ℃/min., and the desorption of NH_3 was recorded with a thermal conductivity detector.

2 Results and discussion

2.1 Effect of HF/HCC-1230za molar ratio and reaction temperature

It is known that HCFO-1233zd (*E*) was synthesized by conducting a fluorination reaction of HF and HCC-240fa in the presence of catalyst Cr_2O_3 at 270 ~ 300 ℃ with the molar ratio of HF/HCC-240fa varied from 20 to 29. Only 82% selectivity to HCFO-1233zd (*E*) is obtained with HF/HCC-240fa molar ratio of 20∶1, at 270 ℃, and at atmospheric pressure[18]. In our work, the reactions of HCC-1230za with anhydrous HF were started first using Zn/Cr_2O_3 catalyst at atmospheric pressure and at 250 ℃. We investigated the effects of molar ratio of HF/HCC-1230za on the selectivity to HCFO-1233zd (*E*). Table 1 shows that the data of product distribution at different molar ratio of HF/HCC-1230za. The conversion of HCC-1230fa increased significantly from 91.0% to 98.8%, and the selectivity to HCFO-1233zd (*E*) increased from 55.2% to 81.5% as the molar ratio of HF/HCC-1230za varied from 6 to 10. At the same time, the selectivity to HCFO-1233zd (*Z*) and HCFO-1232zc decreased drastically from 14.2% to 0.88% and 11.0% to 6.50% respectively. It suggested that the formation of unwanted side products HCFO-1233zd (*Z*) and HCFO-1232zc is greatly suppressed by excess HF (Scheme 2). Even if

Table 1 The effect of HF/HCC-1230za molar ratio on the selectivity to HCFO-1233zd (*E*) [a]

Entry	HF/1230za (mol/mol)	Conversion/% 1230za	Distribution/%[b]				
			1233zd (*E*)	1233zd (*Z*)	1232zc	245fa	other
1	6	91.0	55.2	14.2	11.0	–	10.6
2	8	93.4	61.3	10.5	15.2	–	6.43
3	10	98.8	81.5	0.88	6.50	2.01	7.90
4	12	99.1	80.1	2.90	5.70	0.30	10.1

a. Reaction conditions: at 250 ℃, and with contact time 10 s; b. The distribution of products by GC analysis.

the molar ratio of HF/HCC-1230za further increased beyond 10, little influence on the selectivity to HCFO-1233zd (*E*) and the amount of side products. So we choose HF/HCC-1230za molar ratio of 10 ∶ 1 in the next experiment.

As shown in Table 2, the selectivity to HCFO-1233zd (*E*) increased remarkably with the reaction temperature varied around 200 ℃, and the selectivity

Table 2 The effect of reaction temperature on the selectivity to HCFO-1233zd (*E*)[a]

Entry	Temperature /℃	Conversion/%	Distribution/%[b]				
		1230za	1233zd (*E*)	1233zd (*Z*)	1232zc	245fa	other
1	150	91.6	60.4	1.42	24.5	–	5.28
2	200	99.4	98.2	–	–	1.20	–
3	225	97.9	87.5	0.30	6.90	3.16	0.10
4	250	98.8	81.5	0.88	6.50	2.01	7.90
5	275	97.4	88.1	0.79	6.00	1.02	1.53
6	300	98.1	84.2	1.90	5.10	2.11	4.80

a. Reaction conditions: with HF/HCC-1230za molar ratio of 10 ∶ 1, and with contact time 10 s; b. The distribution of products mby GC analysis.

to HCFO-1233zd (*E*) declined if reaction temperature increase. At this temperature, the conversion of HCC-1230za is also the highest. Whereas, the selectivity to HCFO-1232zc decreased from 24.5% to 5.10% as temperature increased from 150 to 300 ℃. These results indicate that the reaction of HCFO-1232zc with HF is difficult to occur in this reaction because it requires higher energy (Scheme 2). With the reaction temperature increasing from 150 to 300 ℃, HCFO-1233zd (*Z*) firstly decreased and then increased. This means that the reaction temperature has an effect on the transformation between two isomer HCFO-1233zd (*E*) and HCFO-1233zd (*Z*) (Scheme 2)[11].

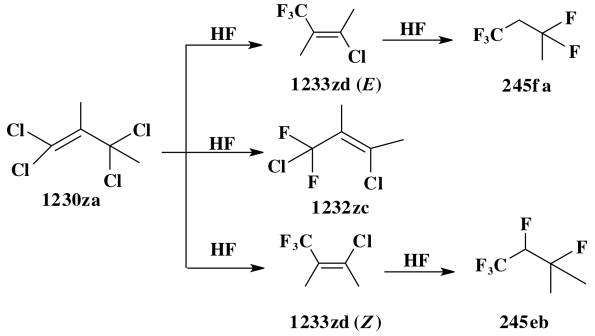

Scheme 2 Products and by-product for the fluorination of HCC-1230za with HF over Zn/Cr_2O_3 catalyst

2.2 Effect of catalyst

Next, we observed the reactions of HCC-1230za with HF using different catalysts and an additional reaction of 10-fold excess HF at 200 ℃. From Table 3, it can be seen that the use of Zn/Cr_2O_3 catalyst resulted in 98.2% of HCFO-1233zd (*E*) (Table 3, entries 3). While the use of $Zn/Al/Cr_2O_3$, $Co/Al/Cr_2O_3$, 4% Zn/2% Cr/γ-Al_2O_3 and 8% Zn/4% Cr/γ-Al_2O_3 catalyst revealed 72.9%, 68.4%, 83.7% and 88.3% of HCFO-1233zd (*E*) respectively (Entries 1, 2, 4, and 5). The catalyst Zn/Cr_2O_3 was more effective in yielding HCFO-1233zd (*E*) and avoiding HCFO-1233zd (*Z*) than other catalysts. Therefore, the addition of Zn^{2+} to Cr_2O_3 significantly increases the selectivity of HCFO-1233zd (*E*) (Table 3, Entry 3).

Because the stability of the catalyst is crucial in practical application[23-26], long term reaction were conducted using the catalysts $Zn/Al/Cr_2O_3$, $Co/Al/Cr_2O_3$, and Zn/Cr_2O_3 at 200 ℃ and contact time 10 s, respectively (Table 3). The conversions remained constant (>99%) and the selectivity of HCFO-1233zd (*E*) gradually declined from 98.2% to 88.2% at a time on stream of 118 h using Zn/Cr_2O_3 catalyst. This indicates that Zn/Cr_2O_3 catalyst is stabled uring the 118 h testing, and the selectivity to HCFO-1233zd (*E*) is satisfactory (Table 3, Entry 3). Using $Zn/Al/Cr_2O_3$ and $Co/Al/Cr_2O_3$ catalysts after 112 and 120 h reaction, the conversions not significantly changed as compared with the initial of 95.2% and 94.3%, and the

Table 3 The reactions of HCC-1230za with HF using different catalysts[a]

Entry	Catalyst	Conversion/%	Distribution/%[b]					Lifespan
		1230za	1233zd (*E*)	1233zd (*Z*)	1232zc	245fa	other	/h
1	$Zn/Al/Cr_2O_3$	95.2	72.9	3.02	13.2	–	6.10	112
2	$Co/Al/Cr_2O_3$	94.3	68.4	4.90	17.0	–	4.04	120
3	Zn/Cr_2O_3	99.4	98.2	–	–	1.20	–	118
4	4% Zn/2% Cr/γ-Al_2O_3	99.8	83.7	5.08	10.0	–	0.50	19.0
5	8% Zn/4% Cr/γ-Al_2O_3	99.9	88.3	5.00	5.70	–	0.88	13.5

a. Reaction conditions: with HF/HCC-1230za molar ratio of 10∶1, at 200 ℃, and with contact time 10 s; b. The distribution of products by GC analysis.

selectivety to HCFO-1233zd (*E*) were 62.9% and 58.4%(Table 3, Entries 1 and 2) respectively. Although 4% Zn/2% Cr/γ-Al_2O_3 and 8% Zn/4% Cr/γ-Al_2O_3 catalysts suffered the most severe deactivation compared with other catalysts, the results of the study demonstrate the beneficial effect of zinc loading to chromium-containing alumina on increasing the selectivity of HCFO-1233zd (*E*) (Table 3, Entries 4 and 5).

The generation of active CrO_xF_y species could be approached by adding Zn^{2+}, Co^{2+} and Al^{3+} in the Cr_2O_3-based catalysts. For example, Lee et al[33] found that MgF_2/ Cr_2O_3 catalyst was more active than Cr_2O_3 catalyst for the synthesis of 1,1,1,2-tetrafluoroethane (HFC-134a) from 2-chloro-1, 1, 1-trifluoroethane (HCFC-133a), which was related to $MgCrO_xF_y$ species generated through the reaction of CrF_3 and MgF_2. The vacant sites of CrF_3 or $CrF_x(OH)_{3-x}$ are believed to be responsible for the L acidity, whereas B acidity can be attributed to the presence of hydroxyl group. Zn/Cr_2O_3 catalyst has the suitable acidity site distribution and strength of B acid and L acid, and which give high stable and selectivity under optimum fluorination conditions.

The reactions of HCC-1230za with HF over Zn/Cr_2O_3 catalyst prepared at different calcination temperature were carried out in N_2 or H_2 atmosphere. In preparation process of the catalysts designed as Zn/Cr_2O_3-350-N_2, Zn/Cr_2O_3-350-H_2, Zn/Cr_2O_3-460-N_2, Zn/Cr_2O_3-460-H_2, Zn/Cr_2O_3-560-N_2, Zn/Cr_2O_3-560-H_2, Zn/Cr_2O_3-600-N_2, and Zn/Cr_2O_3-600-H_2, the precipitated slurry was calcined at 350, 460, 560, and 600 ℃ for 4 h in N_2 or H_2 atmosphere to obtain the final catalysts, respectively. The results are summarized in Table 4. The reaction of HCC-1230za with HF resulted in 81.9% of HCFO-1233zd (*E*) over catalyst

Table 4 The reactions of HCC-1230za with HF using Zn/Cr_2O_3 catalyst prepared at different calcination temperature under H_2 or N_2 atmosphere[a]

Entry	Catalyst	Conversion/%	Distribution/%[b]				
		1230za	1233zd (*E*)	1233zd (*Z*)	1232zc	245fa	other
1	Zn/Cr_2O_3-350-N_2	93.9	81.9	0.20	2.50	–	9.30
2	-H_2	98.0	87.0	5.72	0.56	–	4.70
3	-460-N_2	99.7	87.3	2.19	6.06	–	4.10
4	-H_2	99.4	98.2	–	–	1.20	–
5	-560-N_2	99.1	85.6	6.00	4.60	–	2.90
6	-H_2	99.3	84.0	7.04	4.10	0.80	3.40
7	-600-N_2	97.7	80.0	5.70	6.40	–	5.60
8	-H_2	98.3	82.0	10.1	2.40	–	3.80

a. Reaction conditions: with HF/HCC-1230za molar ratio of 10∶1, at 200 ℃, and with contact time 10 s; b. The distribution of products by GC analysis.

Zn/Cr_2O_3-350-N_2, while 87.0% of HCFO-1233zd (*E*) was gained over catalyst Zn/Cr_2O_3-350-H_2 (Entry 1 vs Entry 2, Table 4). The selectivity of HCFO-1233zd (*E*) steadily increased from 81.9% (at calcined 350 ℃) to 98.2% (at calcined 460 ℃) (Entry 1, 2, 3, and 4, Table 4). While the selectivity decreased from 98.2% to 82.0% (entry 4, 5, 6, 7, and 8, Table 4) if calcination temperature gradually increased to 600 ℃. It can be seen that the calcination temperature has an effect on the selectivity to HCFO-1233zd (*E*), and the catalytic precursor calcined under H_2 was more effective than that under N_2 atmosphere (Entry 3 vs Entry 4, and Entry 5 vs Entry 6, Table 4). These results are consistent with Brunet's[34] and Xie's [35]. Brunet et al [34] investigated the effects of activation temperature and atmosphere (N_2, H_2 or air) of Cr_2O_3 catalyst on the synthesis of HFC-134a from HCFC-133a. They concluded that Cr species of reversible oxidation state are the active sites of reaction. Xie's group demonstrated the calcination temperature have great influence on the crystalline size, surface acid sites and the molar fraction of F in the catalyst[35]. With increasing calcination temperature, Cr_2O_3 translates from amorphous structure into crystalline phase, and the intensity of the diffraction peaks gradually becomes stronger. On the other hand, the molar fraction of F in the catalyst and the amount of surface acid sites decrease with increasing calcination temperature.

2.3 Product distribution studies

Bsed on the obtained products and by-products several plausible reaction pathways (Scheme 2) were inferred. The product HCFO-1233zd (*E*) can be obtained by the fluorination of HCC-1230za with HF in the presence of a suitable catalyst. Of course, this is an oversimplified reaction path that does not fully reflect the actual reactions that may occur under the established catalytic conditions. From Scheme 2, it can be speculated that the actual reaction system may be more complicated when considering the isomers of several possible intermediates. Besides the expected HCFO-1233zd (*E*), the other minor components formed are 1,3- dichloro-3,3- difluoropropene (HCFO-1232zc), and with trace amounts of 1,3,3-trichloro-3-fluoropropene (HCFO-1231zb), 1,3,3-trichloro-1,1-difluoropropane (HCFC-242fb), 3,3-dichloro-1,1,1-trifluoropropane (HCFC-243fc), 1,1,1,2,3-penta- fluoropropane (HFC-245eb), and HFC-245fa in all experiments. The selectivities to the trace amounts and other unknown products are not discussed in this work.

2.4 Characterization of the composite catalysts

XRD analyses were performed to characterize the bulk properties of Zn/Cr_2O_3 catalysts (Fig. 1). The results show that under the preparation conditions of

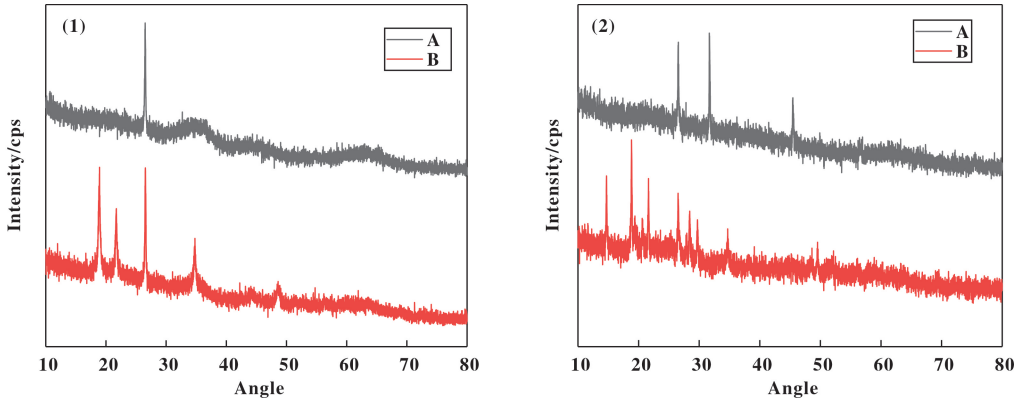

Fig.1 XRD patterns of the catalysts: (1) (A) the fresh catalyst Zn/Cr_2O_3; (B) catalyst Zn/Cr_2O_3 after 118 h reaction, and (2) (A) the fresh catalyst $Co/Al/Cr_2O_3$; (B) catalyst $Co/Al/Cr_2O_3$ after 120 h reaction

Zn/Cr_2O_3 catalyst, the fresh catalyst (Fig.1(1) (a)) is mainly amorphous Cr_2O_3, but it contains microcrystalline phase of Cr_2O_3 with good dispersibility, which size is estimated to be between several nanometers. The XRD pattern shows a diffraction pattern of microcrystalline phase of Cr_2O_3. The maximum peak width at half

height is wider than that of single crystal Cr_2O_3. In the Fig.1(1) (a), 2θ is a peak of graphite at 25.2°, and the 2θ of the diffraction peak of crystalline Cr_2O_3 is 44.4°, while the peaks at 34.4° and 36.2°, 63.2° and 65.0° overlap. However, no diffraction peak related to zinc species such as ZnO could be detected, suggesting the zinc species might be highly dispersed. The XRD pattern of Zn/Cr_2O_3 catalyst after 118 h reaction (Fig. 1(1) (b)) is not significantly changed as compared with the fresh catalyst (Fig.1(1) (a)). The results (Fig.1(1) (a) and (b)) indicated that Zn/Cr_2O_3 catalysts was very stable during the fluorination process. But a new microcrystalline phase of CrF_3 (18.8°, 21.6°, and 34.6°) was found in the Fig.1(1) (b). Although Cho et al[36]. Found that amorphous CrO_3 with high dispersion was more advantage for the fluorination synthesis of HFC-134a from HCFC-133a than the crystalline Cr_2O_3, in our work the XRD results, as well as the evaluation results of Zn/Cr_2O_3 catalyst activity indicate that most of the amorphous Cr_2O_3 and finely dispersed microcrystalline phase of Cr_2O_3 together lead to high activity, high selectivity, and high stability of the catalyst. Catalyst $Co/Al/Cr_2O_3$ after 120 h. Reaction and the fresh one were almost amorphous Cr_2O_3(Fig.1(2) (a) and 1(b)), which again confirmed our results.

The large surface area catalysts are desired in gas phase fluorination synthesis of HFC-134a from HCFC-133a, but the normal fluorinated metal oxides or metal fluorides have a small surface area ($< 50\ m^2 \cdot g^{-1}$)[34]. BET-surface area, pore size and pore volume of the catalyst used here are summarized in Table 5. The

Table 5 The data of BET-surface area, pore size, and pore volume of the catalysts

Entry	Catalyst	$S_{BET}/(m^2 \cdot g^{-1})$	Pore size/nm	Pore volume/($cm^3 \cdot g^{-1}$)
1	Zn/Cr_2O_3	188	5.28	0.249
2[a]	–	448	2.46	0.276
3	$Zn/Al/Cr_2O_3$	182	4.35	0.177
4[b]	–	18.2	3.65	0.017
5	$Co/Al/Cr_2O_3$	169	4.69	0.245
6[c]	–	66.9	2.69	0.045

a. Zn/Cr_2O_3 catalyst after 118 h reaction; b. $Zn/Al/Cr_2O_3$ catalyst after 112 h reaction; c. $Co/Al/Cr_2O_3$ catalyst after 120 h reaction.

specific surface areas are 188, 182, and 169 $m^2 \cdot g^{-1}$ for the fresh Zn/Cr_2O_3, $Zn/Al/Cr_2O_3$, and $Co/Al/Cr_2O_3$ catalysts, respectively. This indicating that the specific surface area of these composite catalysts calcined at 460 ℃ in H_2 atmosphere is larger than the fluorination catalyst already reported. The specific surface area of Zn/Cr_2O_3 catalyst after 118 h reaction is 448 $m^2 \cdot g^{-1}$. However, the specific surface areas are 18.2 and 66.9 $m^2 \cdot g^{-1}$ for $Zn/Al/Cr_2O_3$ after 112 h reaction and $Co/Al/Cr_2O_3$ catalyst after 120 h reaction, respectively. Thus, the conversion of HCC-1230za and the selectivity to HCFO-1233zd (E) are related to the specific surface area of the Zn/Cr_2O_3 catalyst.

XPS spectra were used to identify the surface Cr species of catalyst Zn/Cr_2O_3, $Co/Al/Cr_2O_3$, and $Zn/Al/Cr_2O_3$(Fig. 2). For the fresh Zn/Cr_2O_3 catalyst, two kinds of Cr species can be attributed respectively (Fig.2 (1) (a))[37]. Then, the spectrum of the Cr 2p for Zn/Cr_2O_3 catalyst after 118 h reaction, $Co/Al/Cr_2O_3$ catalyst after 120 h. reaction, and $Zn/Al/Cr_2O_3$ catalyst after 112 h. Reaction became broadening, and were shifted to higher binding energy(Fig.2 (1) (b), (2) (a), and (2) (b)). The broad Cr $2p_{3/2}$ peak of Zn/Cr_2O_3 sample was fitted by three components at 578.6, 579.9 and 582.7 eV, respectively. The peak at 578.6 eV is assigned to the $Cr(OH)_3$ phase. The peak at 579.9 eV is ascribed to the Cr_2O_3 phase. Finally, the weak peak at 582.7 eV is likely due to CrO_xF_y

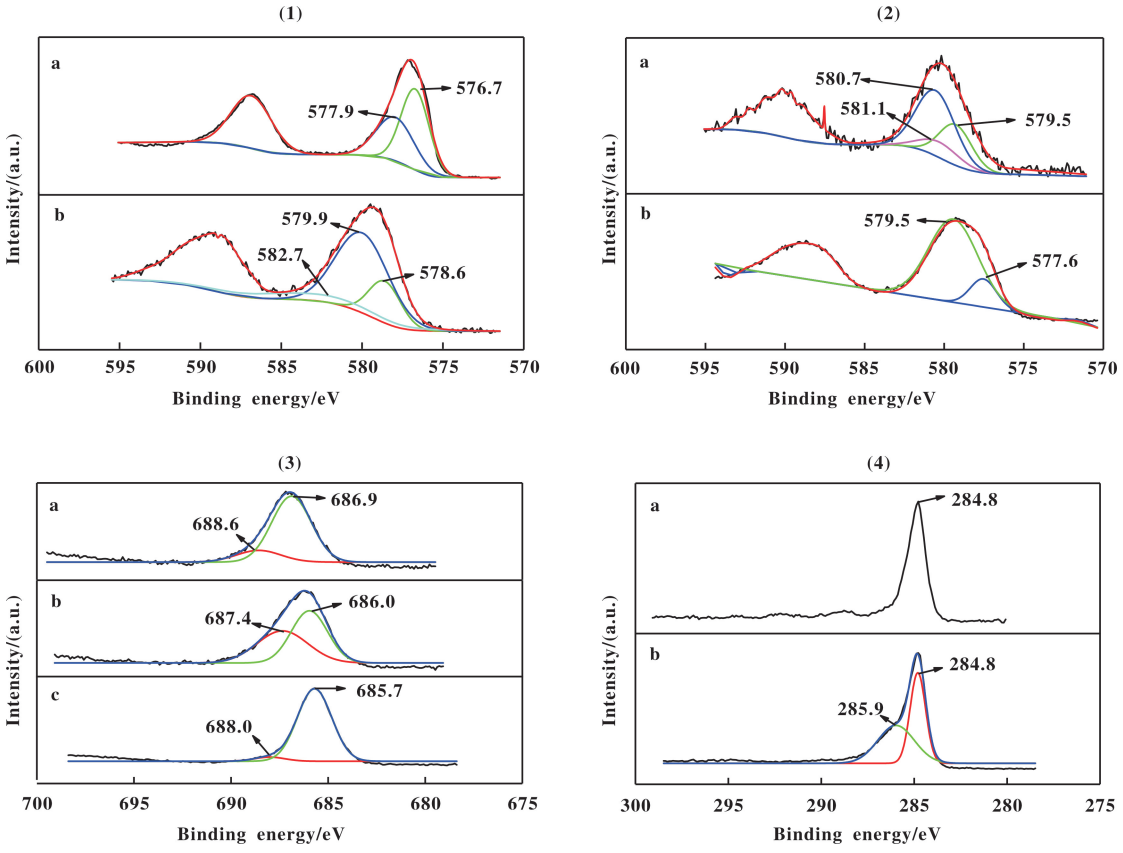

Fig.2 (1) XPS spectra of the Cr 2*p* for Zn/Cr_2O_3 catalysts (a) before and (b) after 118 h, reaction; (2) XPS spectra of the Cr 2*p* for (a) $Co/Al/Cr_2O_3$ catalyst after 120 h, reaction, and (b) $Zn/Al/Cr_2O_3$ catalyst after 112 h, reaction; (3) XPS spectra of the F 1*s* for (a) Zn/Cr_2O_3 catalyst after 118 h, reaction, (b) $Co/Al/Cr_2O_3$ catalyst after 120 h, reaction, and (c) $Zn/Al/Cr_2O_3$ catalyst after 112 h, reaction; (4) XPS spectra of the C 1*s* for Zn/Cr_2O_3 catalysts (a) before and (b) after 118 h reaction.

species[38]. The $Cr(OH)_3$ phase could be formed through the reaction of Cr_2O_3 with hydroxyl or water because the samples were exposed in air before the XPS testing.

The high-resolution F 1*s* core level spectra in Fig. 2 show two peaks at 685.7~686.9 and 687.4~688.6 eV for Zn/Cr_2O_3, $Co/Al/Cr_2O_3$, and $Zn/Al/Cr_2O_3$ catalysts after 118, 120, 112 h, reaction, respectively. The peak at 685.7~686.9 eV in three catalysts indicates the presence of CrF_3. The relatively weaker peak at 687.4~688.6 eV is ascribed to a new chromium fluoride phase CrO_xF_y with higher oxidation states than Cr^{3+}. For Zn/Cr_2O_3 catalyst after 118 h reaction, C 1*s* peaks were deconvoluted into two peaks with binding energies at about 284.8 and 285.9 eV respectively, attributing to the C and $-(CF_3CHCHCl)_n-$. Clearly, carbon deposition over Zn/Cr_2O_3 catalyst after 118 h reaction are higher than that of the fresh Zn/Cr_2O_3 catalyst. Especially, carbon deposition derived from polymerization over Zn/Cr_2O_3 catalyst after 118 h reaction are higher than the fresh Zn/Cr_2O_3 catalyst respectively (based on the $-(CF_3CHCHCl)_n-$) (Fig.2 (4) (a) and (4) (b)). The differences in Cr $2p_{3/2}$, F 1*s*, and C 1*s* core level spectra suggest changes in the catalyst surface properties after/during the reaction, and the exterior Cr_2O_3 were strongly interacted with HF during the vapor fluorination process. Moreover, the presence of CrO_xF_y species is important to the catalytic performance (both activity and selectivity)[37,39-40]. This result was consistent with Blanchard *et al*[41], observation that in a set of temperature-programmed oxidation, the fluorination activity of Cr_2O_3 is

greatly influenced by the presence of Cr in higher oxidation state.

During the fluorination reaction, the Brønsted and Lewis acid site distribution of the catalyst Zn/Cr_2O_3 surface directly affect the catalytic properties of F/Cl exchange reactions[35]. Py-IR spectrum of the catalyst Zn/Cr_2O_3 are shown in Fig.3 (1). It can be observed from Fig.3 that the characteristic peaks of 1466, 1504 and 1556 cm^{-1} on the spectrum belong to the L acid and B acid sites respectively . The absorption peak at

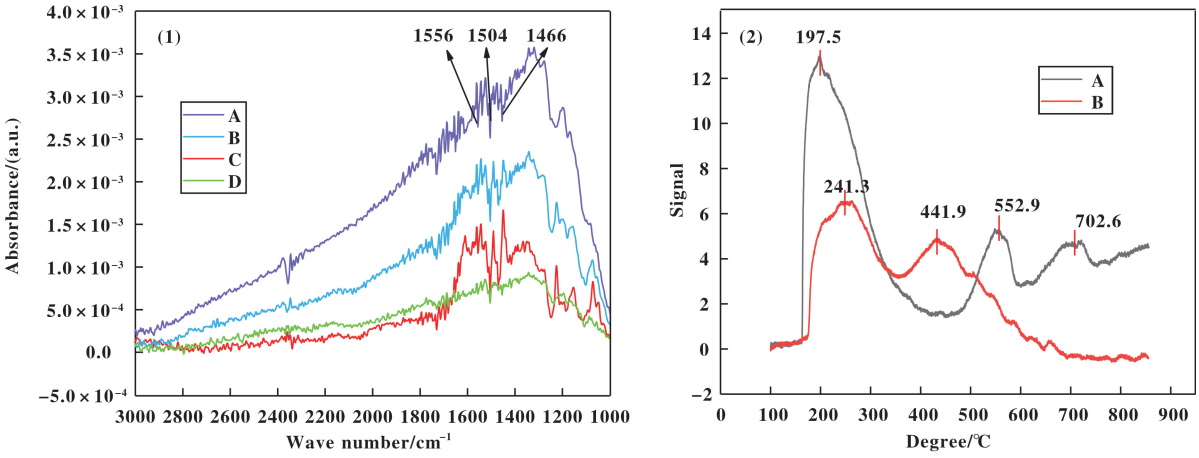

Fig.3 (1) Py-IR spectrum of Zn/Cr_2O_3 catalyst: (a) desorption of pyridine of catalyst after 118 h reaction at 400 ℃, (b) desorption of pyridine of catalyst after 118 h reaction at 150 ℃, (c) adsorption of pyridine of catalyst after 118 h reaction at 150 ℃, (d) adsorption of pyridine of the fresh catalyst at 150 ℃; (2) NH_3-TPD profiles of Zn/Cr_2O_3 catalyst: (a) after 118 h reaction, and (b) the fresh

1466 cm^{-1} is a characteristic peak of the coordination complex of pyridine and Lewis acid site, belonging to the Lewis acid site of the catalyst. The absorption peak at 1556 cm^{-1} is a characteristic peak of pyridinium ions, belonging to the Brønsted acid site of the catalyst. And the absorption peak at 1504 cm^{-1} is a characteristic peak of both the coordination complex of pyridine and Lewis acid site and pyridinium ions, belonging to the Lewis and Brønsted acid site of the catalyst. Comparing Fig.3(1) (a), (b), (c) and (d), it is easy to find that both the catalyst Zn/Cr_2O_3 after 118 h reaction and the fresh catalyst possess the Brønsted and Lewis acid site, and the numbers of acid sites of the catalyst Zn/Cr_2O_3 after 118 h reactionis significantly increased than the fresh catalyst.

The fresh catalyst Zn/Cr_2O_3 and the catalyst after 118 h reaction were characterized by the NH_3-TPD technique (Fig.3 (2)). The NH_3-TPD profiles reveal that for the catalyst after 118 h reaction, three NH_3 desorption peaks were detected with peak temperature at 197.5, 552.9, and 702.6 ℃, respectively, corresponding to the weak and strong acid sites (Fig.3(2), (a)), and for the fresh catalyst shows two broad desorption peaks at temperature range of 190 ~ 550 ℃ (Fig.3(2), b), which suggests that the catalyst contain mild acidic sites. The NH_3 desorption peak at 197.5 ℃ of the catalyst after 118 h, reaction is higher and wilder than the corresponding NH_3 desorption peak at 241.3 ℃ of the fresh catalyst. The two ammonia desorption peaks of the catalyst after 118 h, reaction at 552.9 and 702.6 ℃ are weaker. By contrast, one ammonia desorption peaks of the fresh catalyst at 441.9 ℃ is weaker. This indicates that acidic sites over the catalyst after 118 h reaction are more strong than those over the fresh catalyst. As noted previously, the composite catalyst Zn/Cr_2O_3 after 118 h reaction has suitable acidity sites distribution and strength, and which present high stable and selectivity under optimum fluorination conditions.

3 Conclusion

In summary, the catalyst Zn/Cr_2O_3 is the most effective catalyst among tested catalysts $Zn/Al/Cr_2O_3$, $Co/Al/Cr_2O_3$, 4% Zn/2% Cr/γ-Al_2O_3, and 8% Zn/

4% Cr/γ-Al_2O_3. The addition of Zn^{2+} to Cr_2O_3 significantly increases the selectivity of HCC-1230za with HF to HCFO-1233zd (*E*). The heat treatment conditions in the preparation of the catalyst Zn/Cr_2O_3 has a great influence to the properties of the catalyst. When calcined at 460 ℃ under a H_2 atmosphere, it achieved at 99.4% the conversion of HCC-1230za and 98.2% the selectivity of HCFO-1233zd (*E*). The HCFO-1233zd (*E*) formation can be evidently increased with HF/HCC-1230za (molar ratio of 10 ∶ 1) at 200 ℃. The results of product distribution proved the beneficial effects of molar ratio of reactants and temperature on selectivity to HCFO-1233zd (*E*) using Zn/Cr_2O_3 catalyst. The XRD results of the catalyst Zn/Cr_2O_3 shows that most of the amorphous chromium oxide and finely dispersed microcrystalline phase of Cr_2O_3 together lead to high activity and long lifespan. The conversion of HCC-1230za and the selectivity to HCFO-1233zd (*E*) are related to the specific surface area of the fluorinated catalyst. Also the higher the specific surface area of the catalyst, the higher the catalytic activity and selectivity are. The XPS spectra of the catalyst Zn/Cr_2O_3 probably indicates that the exterior Cr_2O_3 after 118 h reaction were strongly interacted with HF during the fluorination process and formed CrO_xF_y species. The number and strength of Lewis and Brønsted acid sites for the catalyst Zn/Cr_2O_3 after 118 h reaction is significantly increased than the fresh catalysts.

Acknowledgments

This work was supported by Key Research Program of Science and Technology Project of Gansu province (No. 18YF1GA124). We thank Min Deng and Zhao Yanxia for our work.

References:

[1] Zhai Y, Poss A J, Singh R R. Stereoselective synthesis of cis-1-chloro-3, 3, 3-trifluoropropene [J]. *Tetra Lett*, 2016, **57**(3): 396-398.

[2] Li Y C, Luo Z Y. The development of foaming agent for-polyurethane rigid foam and the challenge of HCFC-141bsubstitution[J]. *Poly Indus*, 2014, **29**(5): 1-4.

[3] Engels H W, Pirkl H G, Albers R, *et al*. Polyurethanes: versatile materials and sustainable problem solvers for today's challenges[J]. *Angew Chen Int Ed*, 2013, **52**(36): 9422-9441.

[4] Zheng L F. Some environmental friendly foaming technique of polyurethane foam[J]. *Poly Indus*, 2016, **31**(4): 44-46.

[5] Zhao B, Lu J Y, Mao W. Progress in fluorocarbonblowing agent[J]. *Chem Ind Eng Prog*, 2014, **33**(7): 1864-1870.

[6] Yuan C G, Du C M, Xu H. Properties of rigid polyurethane foam with environmentally friendly blowing agent [J]. *Chin Plastics*, 2014, **28**(2): 45-50.

[7] Hulse R, Singh R, Pokrovski K, *et al*. Converting (E)1-chloro-3,3,3-trifluoropropene into (Z) 1-chloro-3, 3, 3-trifluoropropene, useful as e.g. refrigerants, comprises providing feed stream comprising (E)1-chloro-3,3,3-trifluoropropene and contacting stream with heated surface. US[P], 0152504 A1.

[8] Chen B B, Bonnet P, Elsheikh M, *et al*. Azeotrope-like composition, useful e.g. as heat transfer composition for transferring heat from an article, as a blowing agent, solvent, propellants, and as foamable composition, comprises E-1-chloro-3, 3, 3-trifluoropropene and isopropanol. US[P], 0041529 A1.

[9] Basu R, Cook K, Bement L, *et al*. Azeotrope-like compositions comprising trans-chloro-3, 3, 3-trifluoropropene. US[P], 0102273 A1.

[10] Xiong L Y, Xing Y H, Wang J X. The application of trans-1-chloro-3, 3, 3-trifluoropropene blowing agent in polyurethanerigid foam[J]. *Poly Indus*, 2016, **31**(3): 26-29.

[11] Nair H, Poss A J, Singh R R, *et al*. Process for cis-chloro-2,3,3-trifluoropropene. US[P], 8404907 B2.

[12] Wilmet V, Janssens F. Hydro-fluorination of chlorinated hydrocarbons. US[P], 6362383 B1.

[13] Tung H S, Ulrich K, Merkel D. Low temperature production of 1-chloro-3,3,3-trifluoropropene(HCFC-1233ZD). US[P], 6844475 B1.

[14] Hibino Y, Yoshikaw S, Sakyu F. Production method for 1-chloro-3,3,3-trifluoropropene. US[P], 104039745A.

[15] Wang H Y, Merkel D C. Integrated process to co-produce 1,1,1,3,3-pentafluoropropane, trans-1-chloro-3,3,3-trifluoropropene and trans-1,3,3,3-tetrafluoropropene. CN [P], 103476736A.

[16] Pokrovski K A, Merkel D C. Tong continuous low-temperature process to produce trans-1-chloro-3, 3, 3-trifluoropropene. US[P], 103189339A.

[17] Cottrell S, Tung H S, Pokrovskl K. Integrated process for the production of 1-chloro-3, 3, 3-trifluoropropene. US

[P], 0083316A1.

[18] Tong X S. Vapor phase process for making 1,1,1,3,3-pentafluoropropane and 1-chloro-3,3,3-trifluoropropene. US[P], 5710352.

[19] Yoshikaw S. Method for producing 1, 1, 1, 3, 3-pentafluoropropane. US[P], 6198010B1.

[20] Tatsuo N, Hirokazu A, Akinori Y. Preparation of 1, 1, 1, 3, 3-pentafluoropropyl. US[P], 1206394A.

[21] Satoru Y, Fuyuhiko S, Yasuo H. Manufacture of 1, 3,3, 3-tetrafluoro propene as e.g. protective gas of pharmaceuticals and agrochemicals, involves reacting 1-chloro-3,3, 3-trifluoro propene with hydrogen fluoride in gas phase and in presence of fluorinated catalyst. JP [P], 10067693 A.

[22] Lantz A, Wendlinger L, Requireme B. Synthesis of 1-chloro-3, 3, 3-trifluoropropylene and its fluoridation to 1,1,1,3,3-pentafluoropropylene. US[P], 1166479A.

[23] Merkel D C, Pokrovski K A, Tong X S. Catalyst life improvement for vapor phase manufacture of 1-chloro-3,3, 3-trifluoropropene. US[P], 102933532A.

[24] Yasuo H, Pyouichi T, Shuozou K. Method for producing fluorinated propane. EP[P], 0103578.

[25] a. Lv J, Zhang W, Wang B. Method for producing 1-chloro-3, 3, 3-trifluoropropene. CN[P], 101028994B.

b. Lian Chen-shuai(连晨帅), Dai Rong(代 蓉), Tian Ren(田 韧), *et al.* The effect of preparation method on catalytic properties over Ni-Cu bimetallic catalysts for steam Re forming of ethanol (Ni-Cu 双金属催化剂上乙醇水蒸气重整制氢研究—制备方法对催化性能的影响) [J]. *J Mol Catal*(*China*)(分子催化), 2019, **33**(4): 297-308.

c. Chai Ying-jie(柴应洁), Feng He(冯 鹤), Cui Yan-bin(崔艳斌), *et al.* Structure control of nickel-based perovskite catalyst and its application in methane dry reforming (镍基钙钛矿型催化剂的结构调控及其在甲烷干重整反应中的应用) [J]. *J Mol Catal*(*China*)(分子催化), 2018, **32**(3): 228-239.

[26] Quan H D, Yang H E, Masanori T. Preparation of 1,1, 1, 3, 3-pentafluoropropane (HFC-245fa) by using a SbF5-attached catalyst[J]. *J Fluorine Chem*, 2007, **128**(3): 190-195.

[27] Merkel D C, Pokrovski K A, Tung H S. Azeotropic or azeotrope-like composition used as intermediate for producing fluorinated organic compound e.g. 1-chloro-3,3,3-trifluoropropene, comprises 1,3,3-trichloro-3-fluoroprop-1-ene and hydrogen fluoride. US[P], 0245548.

[28] Merkel D C, Tung H S. Producing 1-chloro-3,3,3-trifluoropropene used as e.g. refrigerant, by dehydrochlorinating 1,1,3,3-tetrachloro-1-fluoropropane in presence of basic solution to form 1, 3, 3-trichloro-3-fluoropropene and fluorinating with hydrogen fluoride. US [P], 0004035.

[29] Bartholomew C H. Mechanisms of catalyst deactivation [J]. *Appl Catal A*, 2001, **212**(1/2): 17-60.

[30] Xu X T, Zhang W X. Kinetics of synthesis of 1,1,1,3,3-pentachloropropane [J]. *CIESC J*, 2014, **65**(1): 176-181.

[31] Boutevin B, Pietrasanta Y, Taha M. Télomères monofonctionnels du chlorure de vinyle—I: Synthèse et caractérisation d′étalons de télomères du chlorure de vinyle[J]. *Eur Polym*, 1982, **18**(8): 675-678.

[32] Kotora M, Hajek M. Selective additions of polyhalogenated compounds to chlogo substituded ethenes catalyzed by a copper complex[J]. *React Kinet Catal Lett*, 1991, **44**(2): 415-417.

[33] Lee H, Jeong H D, Chung Y S, *et al.* Fluorination of CF_3CH_2Cl over Cr-Mg fluoride catalyst: The effect of temperature on the catalyst deactivation [J]. *J Catal*, 1997, **169**(1): 307-316.

[34] Brunet S, Requieme B, Matouba E, *et al.* Characterization by temperature-programmed reduction and by temperature-programmed oxidation (TPR-TPO) of chromium (Ⅲ) oxide-based catalvsts: Correlation with the catalytic activity for hydrofluoroalkane synthesis [J]. *J Catal*, 1995, **152**(1): 70-74.

[35] Xie Z, Fan J, Cheng Y, *et al.* Cr_2O_3 catalysts for fluorination of 2-chloro-3,3,3-trifluoropropene to 2,3,3,3-tetrafluoropropene[J]. *Indus Eng Chem Res*, 2013, **52**(9): 3295-3299.

[36] Cho D H, Kim Y G, Chung M J, *et al.* Preparation and characterization of magnesia-supported chromium catalysts for the fluorination of 1,1,1-trifluoro-2-chloroethane (HCFC-133a) [J]. *Appl Catal B*, 1998, **18**(3/4): 251-261.

[37] Chung Y S, Lee H, Jeong H D, *et al.* Enhanced catalytic activity of air-calcined fluorination catalyst [J]. *J Catal*, 1998, **175**(2): 220-225.

[38] Loustaunau A, Fayolle-Romelaer R, Celerier S, *et al.* Catalytic fluorination of various chlorinated hydrocarbons by HF and a chromium based catalyst: Effect of the presence of zinc[J]. *Catal Lett*, 2010, **138**(3/4): 215-223.

[39] Adamczyk B, Boese O, Weiher N, *et al.* Fluorine modified chromium oxide and its impact on heterogeneously

catalyzed fluorination reactions[J]. *J Fluorine Chem*, 2000, **101**(2): 239-246.

[40] Cheng Y X, Fan J L, Xie Z Y, *et al*. Effects of M-promoter (M=Y, Co, La, Zn) on Cr_2O_3 catalysts for fluorination of perchloroethylene[J]. *J Fluorine Chem*, 2013, **156**: 66-72.

[41] Barrault J, Brunet S, Requieme B, *et al*. Preparation of substitutes for CFCs catalytic properties of chromia for halogen exchange involving hydrogen fluoride and trifluorochloroethane[J]. *J Chem Soc Chem Comm*, 1993, **4**: 374-375.

改性三氧化二铬催化 1,1,3,3-四氯丙烯氟化高选择性合成反式-1-氯-3,3,3-三氟丙烯研究

田　密[1,3], 高　平[2], 张荣慧[1,3], 王来来[1*], 周旺鹰[4], 谢文健[4]

(1. 中国科学院兰州化学物理研究所 羰基合成与选择氧化国家重点实验室, 甘肃兰州 730000;
2. 中国科学院兰州化学物理研究所 固体润滑国家重点实验室, 甘肃 兰州 730000;
3. 中国科学院大学, 北京 100039;
4. 江苏理文化工有限公司, 江苏 常熟 215536)

摘要: 反式-1-氯-3,3,3-三氟丙烯(HCFO-1233zd(*E*))是近年来正在研发的第 4 代发泡剂, 其大气臭氧消耗潜能值为 0.000 24, 温室效应潜能值为 7.0, 毒性低, 常态下不燃, 使用安全; 它也是合成含氟精细化工品的中间体, 以及合成氟树脂和氟弹性体的单体. 我们制备了 Al, Zn, Co 改性的 Cr_2O_3 催化剂, 将其成功应用于 1,1,3,3-四氯丙烯(HCC-1230za)与氟化氢反应中, 高选择性地合成 HCFO-1233zd(*E*), 复合催化剂 Zn/Cr_2O_3 显示高稳定性, 其中 HCC-1230za 转化率高达 99.4%, HCFO-1233zd(E)的选择性高达 98.2%. 反应条件诸如反应物 HF/HCC-1230za 的摩尔比和反应温度等对产物分布有显著影响. 在相对较低的温度(200 ℃)和较大的 HF/HCC-1230za 摩尔比(10∶1)下, 对 HCFO-1233zd(E)的选择性有利. 通过 XRD, XPS, BET 和 V70 吡啶吸附红外光谱技术对复合催化剂Zn/Cr_2O_3进行了表征. XRD 结果表明, 催化剂中大多数无定形 Cr_2O_3 和高度分散微晶相 Cr_2O_3 共同导致催化剂的高活性和高稳定性. HCC-1230za 的转化率与预氟化处理催化剂 Zn/Cr_2O_3 的比表面积有关, 催化剂的比表面积越高, 催化活性越高. XPS 光谱表明, 在预氟化过程中, 表面铬氧化物可能与 F 原子强烈相互作用, 从而导致 Cr 原子的化学环境发生广泛变化. V70 吡啶吸附红外光谱和氨-程序升温脱附技术结果证明尚未失活的催化剂 Lewis 酸和 Brønsted 酸中心的数目和强度与新制备的催化剂相比明显提高.

关键词: 氟化; 1,1,3,3-四氯丙烯; 氟化氢; 反式-1-氯-3,3,3-三氟丙烯; 氟化三氧化二铬